*Solid State Phenomena*
*ISSN: 1662-9779, Vol. 390, pp 137-143*
*doi:10.4028/p-6Mmgit*

*Submitted: 2026-01-19*
*Revised: 2026-02-23*
*Accepted: 2026-02-24*
*Online: 2026-04-17*

# How to Take the Lüders Plateau into Account in the Formability Prediction of Steel Sheets

Lemoine Xavier[1,a*]

[1]Global R&D ArcelorMittal Maizières, voie Romaine, BP30320, F-57283 Maizières-lès-Metz, France

[a*]xavier.lemoine@arcelormittal.com

**Keywords:** lüders, hardening law, formability, steels.

**Abstract.** Some steels exhibit the Lüders effect. This phenomenon depends on the material and structure (test piece geometry, loading speed, etc.). Most work hardening laws do not take this phenomenon into account. The objective of this work is to define the most appropriate hardening law to capture the characteristics of Lüders effects. First, the various aspects of the Lüders effect are presented. Several local hardening laws are proposed to describe the presence or absence of a plateau, some of which are taken from the literature. Simulations of uniaxial tensile tests and stamped-part forming are performed to compare the ability of these different hardening laws to predict the Lüders effect. The Exp_Swift hardening law is recommended for forming cards because it is fully compatible with all the finite element codes dedicated to steel sheet formability analysis and does not require inverse calibration during identification to accurately predict the plateau length.

## Introduction

The Lüders phenomenon is observed as a plateau of nearly constant stress occurring at the onset of plastic deformation, immediately beyond the elastic limit (Fig.1) [1]. It occurs when the stress reaches a maximum value, called the Upper Yield Stress (UYS), before dropping abruptly to a nearly constant level known as the yield plateau stress. The minimum value of the plateau and the length of the Lüders plateau are referred to as the Lower Yield Stress (LYS) and the Yield Plateau Elongation (YPE), respectively. The over-stress peak, together with the constant-stress plateau, distinguishes steels that exhibit a yield plateau from those that do not.

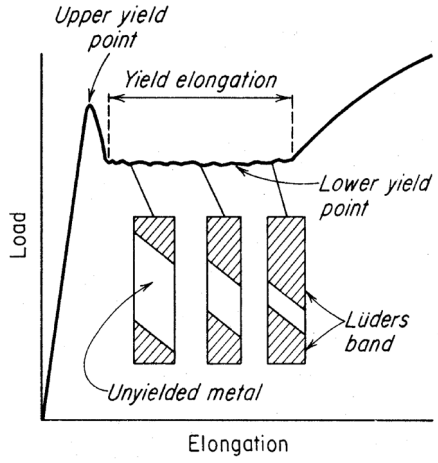


**Fig. 1.** Lüders characterization issued tensile test [1].

The origin of this behavior lies at the atomic scale, specifically in the dislocation mechanisms within the material [2]. Certain dislocations are pinned by Cottrell atmospheres, and their unpinning requires more energy than moving an unpinned dislocation, which explains the observed over-stress at the elastic limit. During the uniaxial tensile test, this disturbance manifests on the specimen as one or several narrow bands of plastic deformation inclined at approximately 55°, propagating through the surrounding material that remains elastically deformed. The localized plastic deformation within

the Lüders band propagates [3], causing a local temperature to increase due to the energy released during dislocation motion, in contrast to elastic deformation. Consequently, thermal imaging is an effective method for visualizing these bands [4].

The characteristics of the Lüders plateau result from an interaction between the intrinsic behavior of steel and the conditions under which the tensile test is performed. The values of UYS, LYS and YPE, depend on the number of pinned dislocations, the concentration of elements (C, N, etc.) forming Cottrell atmospheres [5], the sheet thickness [6], the specimen geometry (the length of the specimen's gauge section), the loading rate [7, 8], and the temperature [9] during the tensile test. Depending on the type of loading path (shear, plane tension, wide tension, rolling, etc.), the Lüders plateau may or may not appear [10].

The inclination of the Lüders band, approximately 55° [11], is identical to that of the shear-localization band responsible for localized necking. Shear bands, like the Lüders plateau, originate from the formation of dislocation cells constrained by the same close-packed planes of the body-centered cubic (BCC) crystal structure of iron atoms in low-carbon steels. A priori, these two phenomena are considered independent of each other in the context of tensile testing of steel sheets.

In forming predictions for steel sheets (such as formability analysis), most hardening laws do not account for this phenomenon. Models incorporating the Lüders effect have primarily been developed for fundamental understanding rather than practical application. The objective of this work is to identify the hardening law most suitable for forming prediction, in order to capture the characteristics associated with Lüders effects.

## Flow Curves of Seven Hardening Laws Used in Finite Element Code

Flow curves of seven hardening laws (Fig. 2) were considered to study the impact of the Lüders plateau on rheology and formability predictions. The hardening law defines the stress–strain curve applied at each integration point and reflects the behavior of a material point. The structural aspect of the Lüders plateau (e.g., the Yield Point Elongation, YPE) predicted by certain hardening laws is obtained directly from simulation.

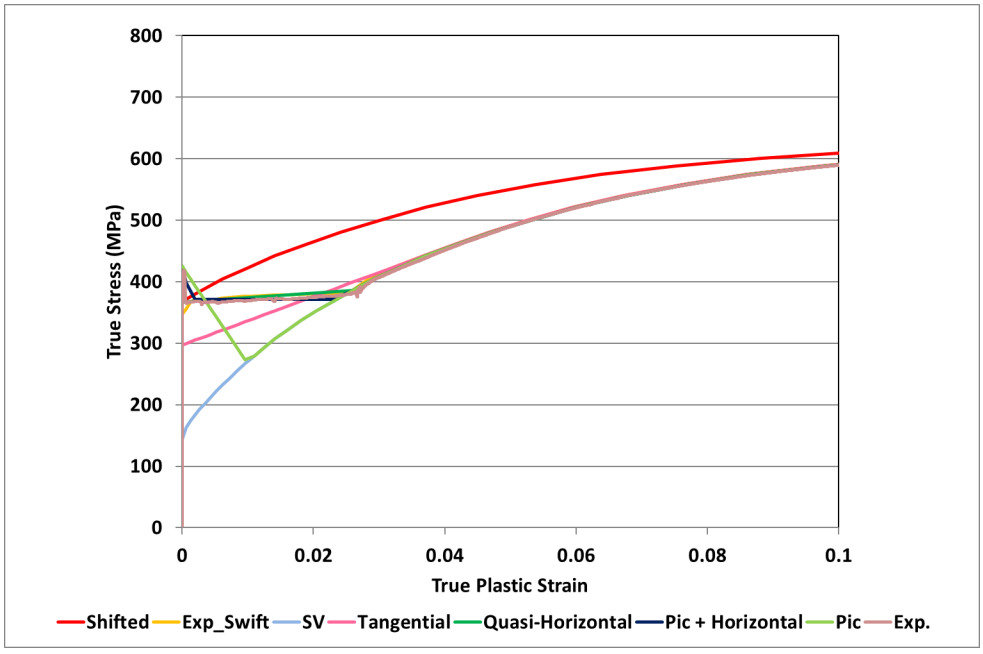


**Fig. 2.** Flow Curves of Seven Hardening Laws for an HSLA steel.

The first hardening law considered is the linear combination of the Swift and Voce models (Eq. 1) [12] referred to as 'SV'. This model does not exhibit a Lüders plateau and will serve as the reference for comparison in forming predictions.

$$\sigma = \alpha \left[ \sigma_0 + R_{sat} \left(1 - exp(- C_r \varepsilon)\right)\right] + (1-\alpha) \left[ K \left( \varepsilon_0 + \varepsilon\right)^n\right]. \quad (1)$$

Here σ and ε denote the true stress and true plastic strain, respectively, while the remaining terms represent material-specific parameters. These material parameters were identified from the section of the tensile curve between the Lüders plateau and the onset of uniform elongation, using Considère's criterion to extrapolate the curve beyond the uniform elongation point [12].

Two other hardening laws do not exhibit any characteristics of the Lüders plateau. The "Shifted" law was previously used because it aimed to capture only the intrinsic behavior of steel, without any interaction with structural effects, which is not the case for the Lüders plateau. The "Tangential" law is a Swift–Voce model, identified over the entire tensile curve, including the Lüders plateau.

The other hardening laws were derived from this "SV" law except for "Exp_Swift", in order to reproduce specific aspects of the Lüders plateau:

- only the plateau itself (YPE), without the upper yield point (UYS) and with slopes that are nearly horizontal ("Exp_Swift" and "Quasi-Horizontal"),
- or including the upper yield point (UYS), as in the model proposed by H. Tsukahara et al. [13] ("Pic"), or through a combination of two laws ("Pic + Horizontal").

The "Exp_Swift" law consists of experimental data points up to the uniform elongation UE, followed by a Swift law beyond UE, whose Swift parameters are derived from the Considère criterion. The "Quasi-Horizontal" law is obtained by adding a quasi-horizontal plateau to the SV law. In this case, the Swift and Voce parameters are approximated as accurately as possible after the Lüders plateau up to UE, and beyond UE the linear-combination parameter between Swift and Voce is determined from the Considère criterion. "Exp_Swift" is the law recommended for achieving an accurate plastic stress–strain relationship under large deformations [12].

All the finite element codes used for the forming of steel sheets enforce a monotonically increasing evolution of plastic strain. Most of these codes allow for a decrease in the engineering stress, whereas some enforce that this stress remains strictly increasing (e.g., "AutoForm®"). This implies that some of these seven work-hardening laws cannot be utilized by this type of finite element code (Table 1).

**Table 1.** Compatibility of Seven Hardening Laws with Four Finite Element Codes.

| | SV | Shifted | Tangential | Exp_Swift | Quasi-Horizontal | Pic | Pic + Horizontal |
|---|---|---|---|---|---|---|---|
| Abaqus® | X | X | X | X | X | X | X |
| PamStamp® | X | X | X | X | X | X | X |
| Ls-Dyna® | X | X | X | X | X | X | X |
| Autoform® | X | X | X | X | X | | |

## Tensile Tests Predictions

The first numerical experiment consists of simulating a tensile test on an ISO 20×80 specimen to determine whether the mechanical characteristics associated with the Lüders plateau can be accurately predicted. The simulation was carried out using Ls-Dyna® with 2×2 mm² shell elements, and each strain-hardening law was implemented via a tabulated input within material model MAT_122, combined with a Hill 48 yield surface identified using three Lankford coefficients (r0=0.9, r45=1, r90=0.7). The loading condition is implemented as a prescribed displacement applied to a set of nodes at the top of the specimen, while another set of nodes at the bottom is fully constrained in both translational and rotational degrees of freedom. The tensile force is computed by averaging the element forces within the central section of the specimen, which is perpendicular to the loading direction. The elongation is then derived using an initial gauge length of 80 mm.

Fig.3 provides the engineering stress–strain representation of the input curve derived from Fig.2 for the three hardening laws ("SV", "Exp_Swift", and "Pic"). It also includes the tensile test response predicted by LS-Dyna®, which is compared with the corresponding experimental curve. From these engineering curves, the mechanical properties—UYS, LYS, YPE, UTS, and UE—were extracted and are reported in Table 2.

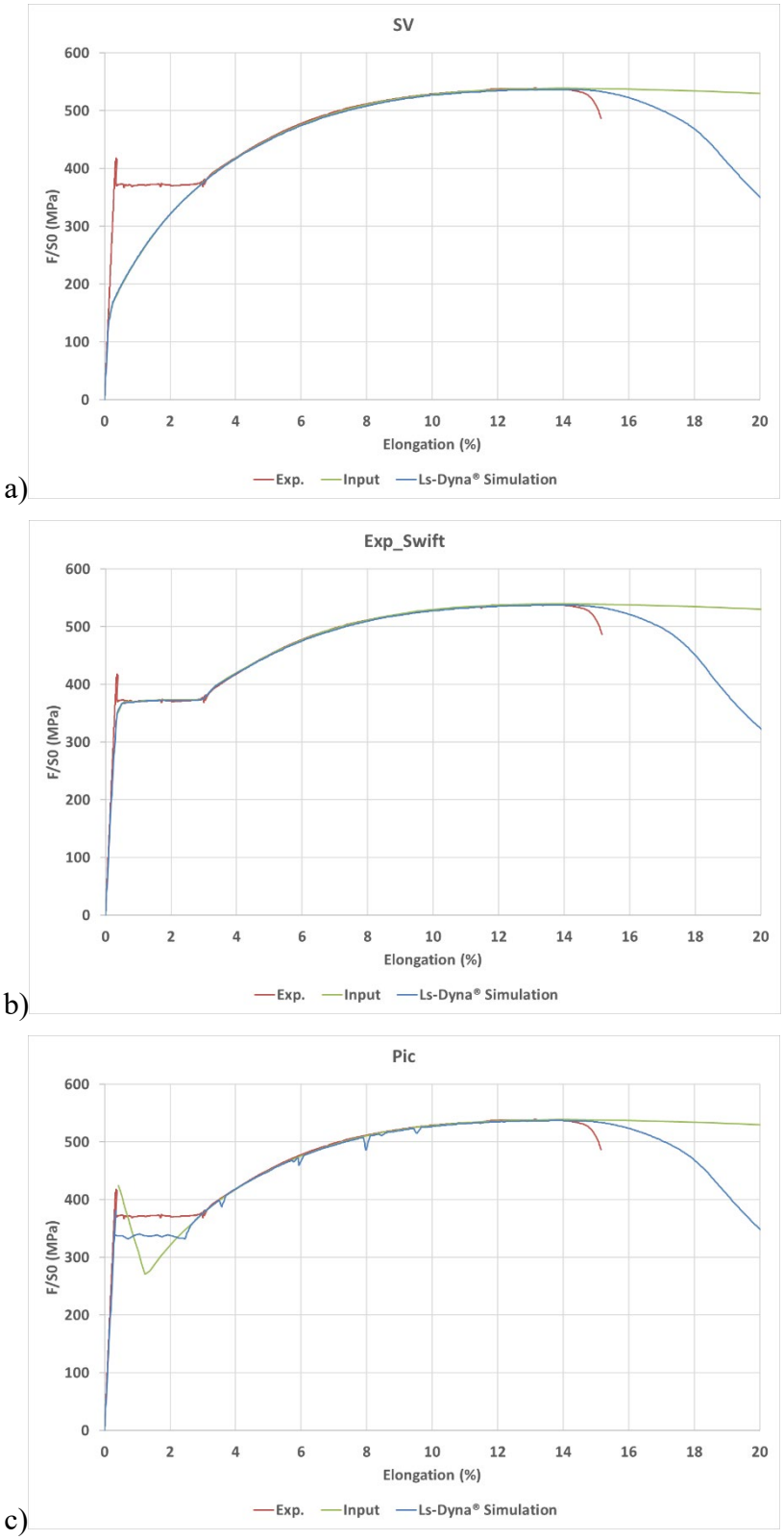


**Fig. 3.** Comparison of flow curves from the experimental test, the prediction by Ls-Dyna®, and Input curve for three hardening laws: SV (a), Exp_Swift (b), Pic (c).

For hardening laws without a plateau, the prediction of the LYS value is inaccurate, and the shifted law further leads to an unrealistically low uniform elongation.

In Table 2, the presence or absence of Lüders band propagation is reported and illustrated in Figure 4 for the "Pic" hardening law. The occurrence of this propagation is exclusively ascribed to the incorporation of UYS in the input hardening law. The predicted UYS values are significantly lower than the experimental ones and those from the input curve ("Pic" and "Pic-Horizontal"), a discrepancy

that is linked to the frequency at which the simulation results were recorded. Achieving a plateau length for both hardening laws that better matches the experimental value requires a recalibration of the input curve and is expected to be influenced by the mesh size.

The advantage of plateau-type laws without UYS ("Exp_Swift" and "Quasi-horizontal") is that both the plateau length and the LYS predicted by the simulation match exactly the input curve (Fig.3b for "Exp_Swift" law).

**Table 2.** Comparison of the predicted mechanical properties of seven hardening laws with experimental values, and presence of band propagation.

| | UYS (MPa) | LYS/YS (MPa) | YE (%) | UTS (MPa) | UE (%) | Band Propagation |
|---|---|---|---|---|---|---|
| Exp. | 418 | 362 | 2.8 | 539 | 12.9 | Yes |
| SV | - | 190 | - | 537 | 13.2 | No |
| Shifted | - | 370 | - | 550 | 10.0 | No |
| Tangential | - | 305 | - | 538 | 13.3 | No |
| Exp_Swift | - | 369 | 2.5 | 538 | 13.4 | No |
| Quasi-Horizontal | - | 367 | 2.6 | 537 | 13.5 | No |
| Pic | 382 | 330 | 2.1 | 537 | 13.9 | Yes |
| Pic + Horizontal | 387 | 368 | 2.8 | 537 | 13.4 | Yes |

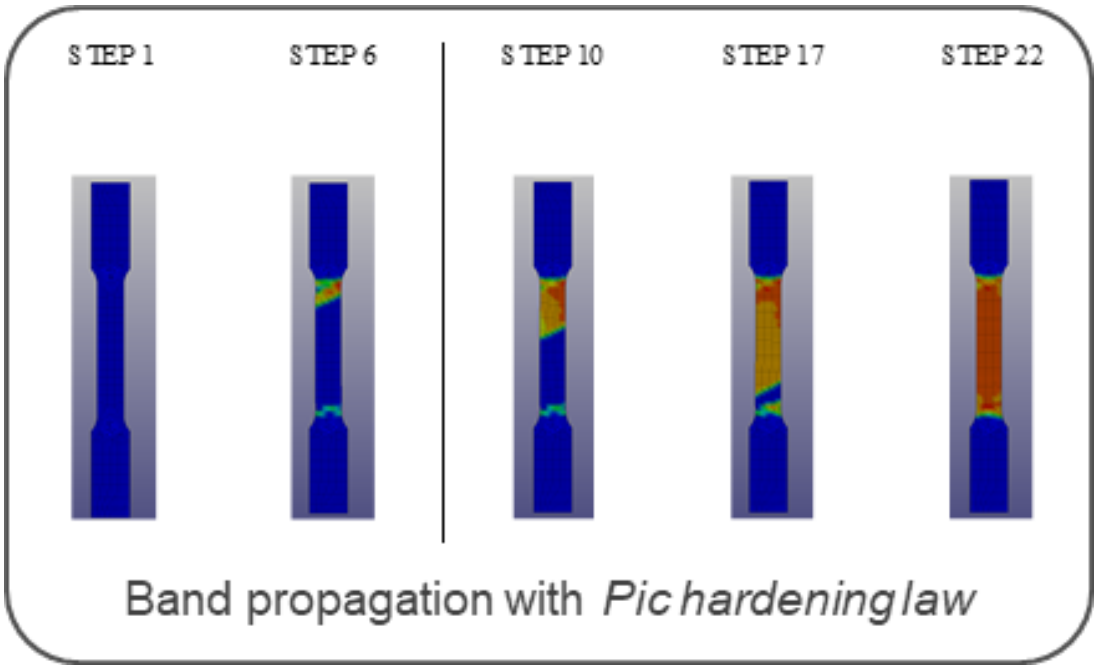


**Fig. 4.** Band propagation with the "Pic" law.

### Stamping Parts Predictions

To investigate the impact of these seven laws on the prediction of formability in stamped parts, several cases were analyzed, all leading to broadly similar conclusions. Accordingly, only the results of hemispherical stamping tests are presented in the following section.

Except for the "Shifted" hardening law, the formability prediction (Fig.5) and Punch force prediction (Fig.6) are comparable to those obtained with the "Exp_Swift" hardening law.

The "Pic" hardening law enables the prediction of band propagation consistent with the experiment (Fig.7). However, this numerical capability can only be achieved when an extremely fine mesh is employed, which is no longer feasible for industrial applications due to the prohibitive computational cost.

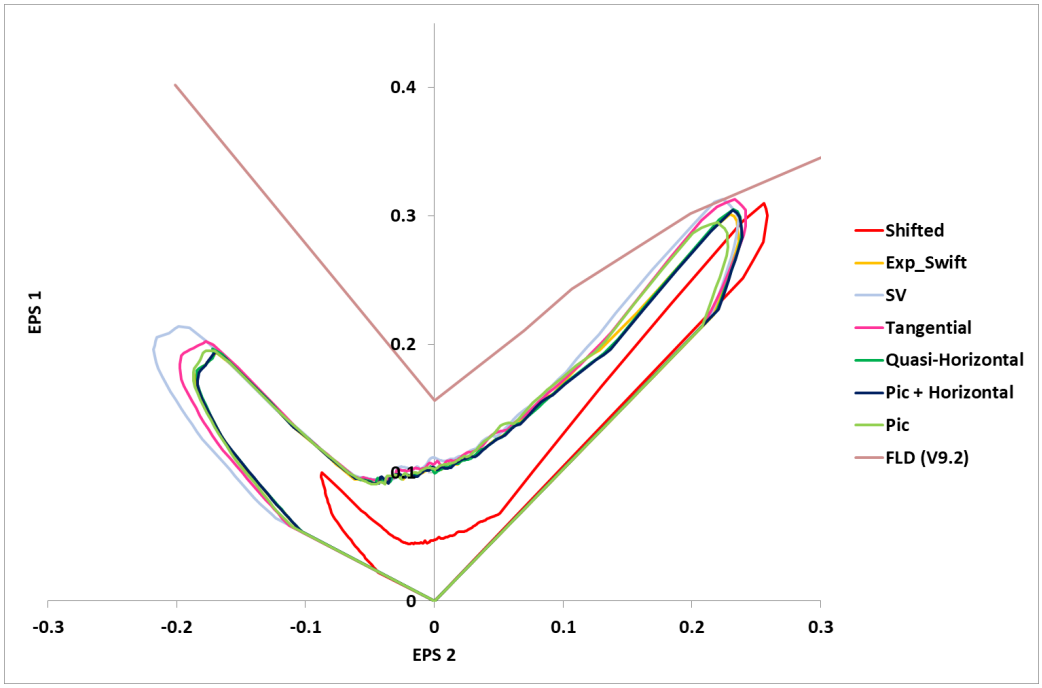


**Fig. 5.** Forming limit diagram of hemispherical stamping tests for seven hardening laws.

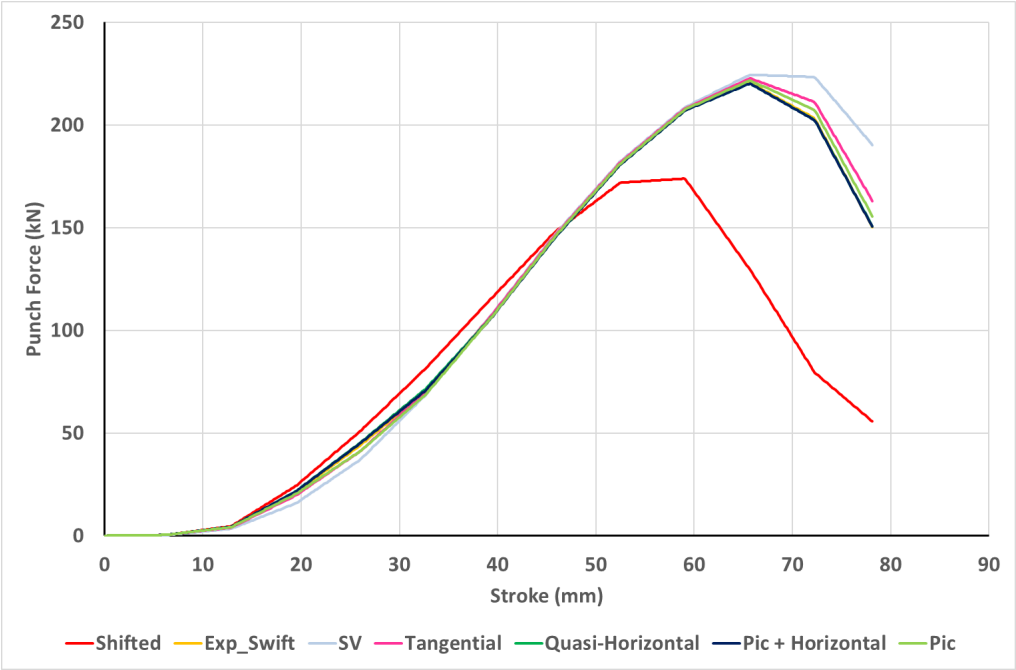


**Fig. 6.** Punch force of hemispherical stamping tests for seven hardening laws.

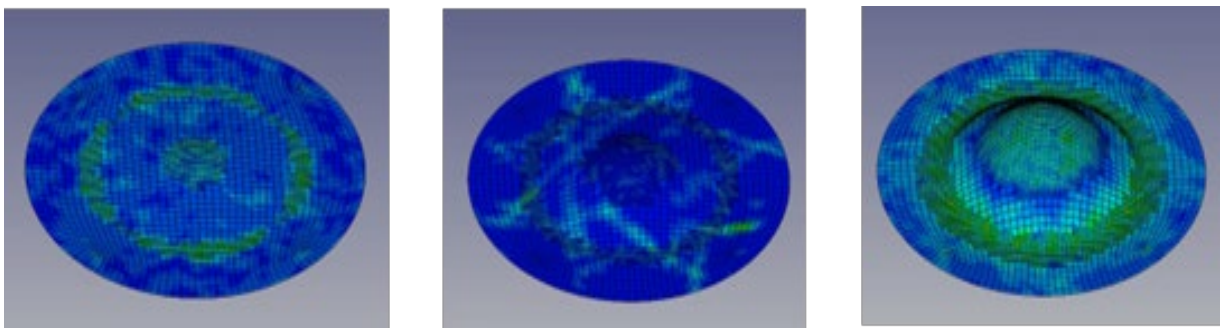

**Fig. 7.** Bands propagation with Pic hardening law appears in intermediate step.

## Conclusion

The recommended hardening law for forming cards is the “Exp_Swift” law, as it is compatible with all the finite element codes dedicated to steel-sheet formability and does not require inverse adjustment during identification to accurately predict the plateau length (Fig.3b), regardless of mesh size. This constitutive law makes it possible to reproduce the mechanical properties guaranteed in the customer’s specification when simulating a tensile test, while satisfying the monotonic stress-increase condition imposed by AutoForm®.

## References

[1] K.H. Subramanian, A.J Duncan. Tensile Properties for Application to Type I and Type II Waste Tank Flaw Stability Analysis(U), WSRC-TR-2000-00232, Westinghouse Savannah River Company, Aiken: SC, 2000.

[2] A.H. Cottrell, B.A. Bilby. Dislocation Theory of Yielding and Strain Ageing of Iron. Proc. Phys. Soc. A 62 (1949), 49-62.

[3] W. Lüders, Über die Äusserung der Elasticität an stahlartigen Eisenstäben und Stahlstäben, und über eine beim Biegen solcher Stäbe beobachtete Molecularbewegung. Dinglers Polytech, jahrgang 5, (1860), 18–22.

[4] H. Louche, A. Chrysochoos. Thermal and dissipative effects accompanying Lüders band propagation. Materials Science and Engineering A307 (2001) 15–22.

[5] J. Winlock. The influence of the rate of deformation on the tensile properties of some plain carbon sheet steels. J. Metals, 5 (1953) 797–803.

[6] X. Jiang, H. Wu, W. Sun, R. Li, M. Chen. Specimen size effect on the lüders deformation in mild steel sheet. Materials Today Communications 44 (2025) 112026.

[7] H. Fujita, S. Miyazaki. Lüders deformation in polycrystalline iron. Acta Metall., 26 (1978) 1273–1281.

[8] V. Ballarin, M. Soler, A. Perlade, X. Lemoine, S. Forest Mechanisms and Modeling of Bake-Hardening Steels: Part I. Uniaxial Tension. Metall. Mater. Trans. A, 40A (2009), 1367-1374.

[9] X. Wang, M. Huang. Temperature dependence of Lüders strain and its correlation with martensitic transformation in a medium Mn transformation induced plasticity steel. Journal of Iron and Steel Research, International 24 (2017) 1073-1077.

[10] M. Mazière, C. Luis, A. Marais, S. Forest, M. Gaspérini. Experimental and numerical analysis of the Lüders phenomenon in simple shear. Int. J. solids and Strec. 106_107 (2017), 305-314.

[11] J. Zhang, Y. Jiang. Lüders bands propagation of 1045 steel under multiaxial stress state. Int. J. Plasticity 21 (2005) 651–670.

[12] X. Lemoine, R. Munier, X. Bellut. A robust identification protocol of flow curve adjusting parameters using uniaxial tensile curve. Material Forming - ESAFORM 2024, Materials Research Proceedings 41 (2024) 2210-2219.

[13] H. Tsukahara, T. Iung. Finite element simulation of the Piobert–Lüders behavior in an uniaxial tensile test. Mater. Sci. Eng. A 248 (1998) 304-308.